

Amplified fluorescence by carbon nanotube (CNT)-assisted surface
plasmon coupled emission (SPCE) and its biosensing application

Kai-xin Xie*, Shu-shu Jia, Jin-hua Zhang, Huan Wang, Qiang Wang

Department of Chemistry, Taiyuan Normal University, Jin zhong 030619, PR China

1. The angular distribution for CNT-assisted SPCE.

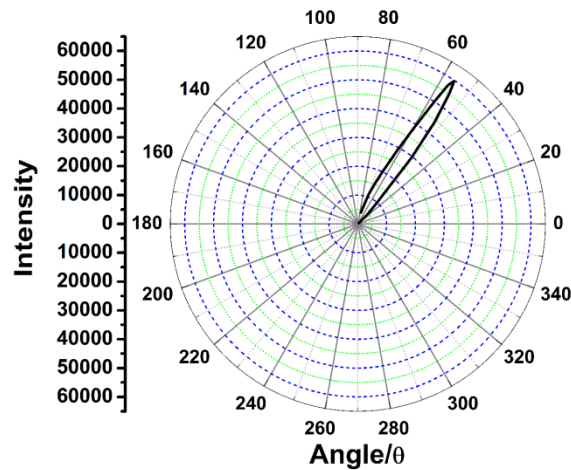


Fig. S1. The angular distribution for CNT-assisted SPCE.

2. The polarization property and the angular distribution of normal SPCE signal.

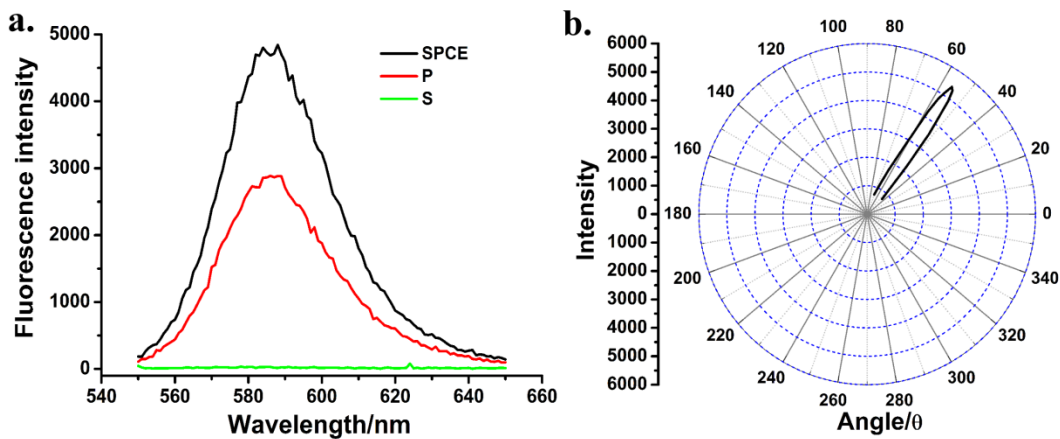


Fig. S2. (a) The polarization property and (b) the angular distribution of normal SPCE signal.

3. The polarization of the fluorescence obtained from the quartz glass substrate modified with and without CNTs.

For the preparation of the quartz glass modified with CNTs, the quartz glass was activated and hydroxylated by immersing into H_2SO_4/H_2O_2 (volume ratio of 7:3), then silanized by a 1% aminopropyltriethoxysilane (APTES, Acros Organics, China) ethanol solution for 1 h to obtain an amine-modified quartz glass. Subsequently, the quartz glass was immersed in a CNT solution for 5 h. Next, the CNT-covered glass was thoroughly rinsed with ultrapure water and dried in air. Afterwards, 1 mM RhB-1% PVA was spin-coated onto the glass at 4000 rpm for 40 s and dried in air to obtain the dye-doped quartz glass. For comparison, 1 mM RhB-1% PVA was deposited on quartz glass without CNTs directly by spin-coating.

4. Fluorescence spectra of fluorophore eluent

1mM RhB-1% PVA was deposited on gold substrate with CNTs by spin-coating. For comparison, 1mM RhB-1% PVA was deposited on gold substrate without CNTs directly by

spin-coating. These two substrates were ultrasonic wash in ultrapure water, and then the fluorescence spectra of the eluents were investigated. The results are shown below.

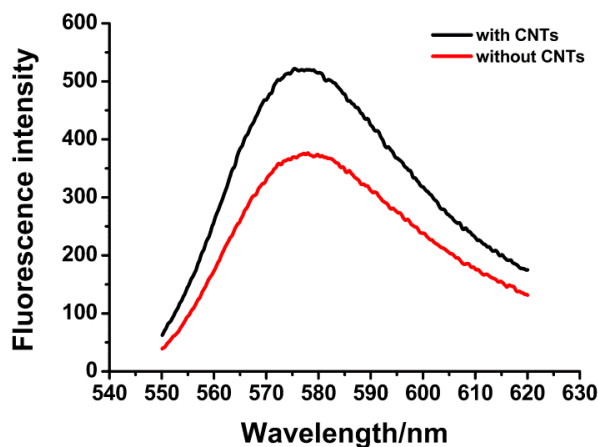


Figure S3. The fluorescence spectra of the eluents of RhB deposited on the substrate with and without CNTs.

5. The enhancement effect of CNTs modification by spin-coating method.

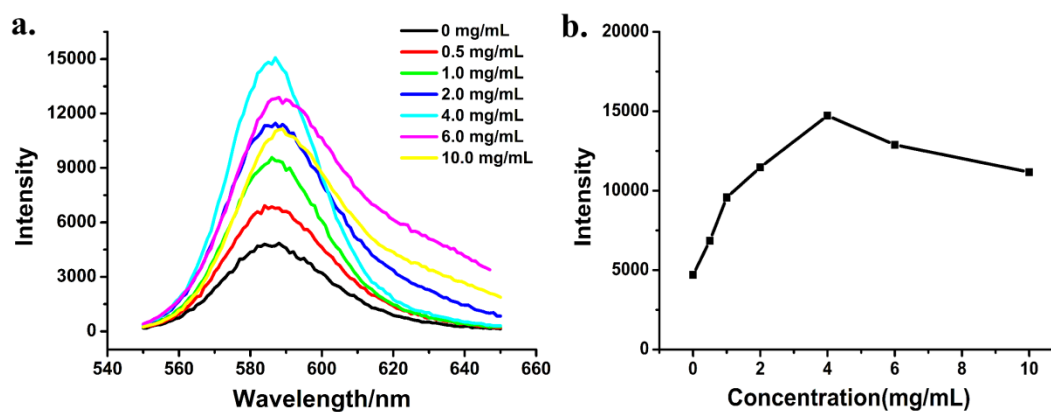


Fig. S4. (a) The spectra for different mixture concentrations of CNTs in 1 mM RhB-1% PVA solution. (b) The relationship between mixture concentration and SPCE intensity.

6. The spectra for different modification concentrations of CNT assistance.

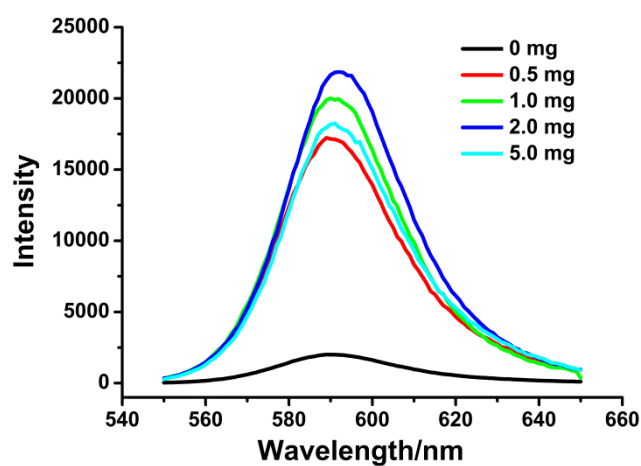


Fig. S5. The spectra for different modification concentrations of CNT.

7. The surface coverage for different modification concentrations of CNT on gold film.

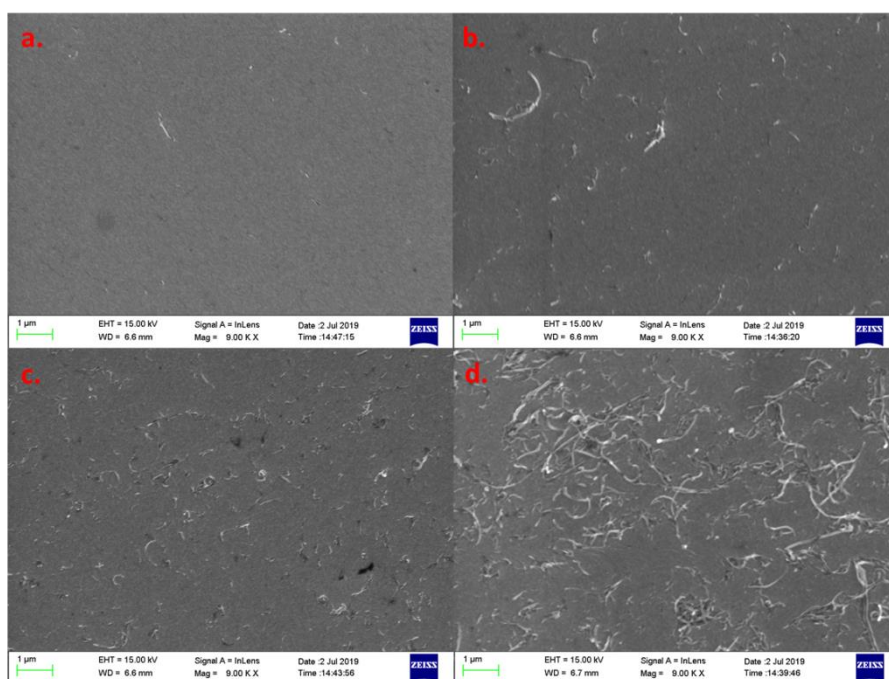


Fig. S6. The SEM images for different modification concentrations of CNT (a-d: 0.5, 1.0, 2.0, 5.0 mg/mL).

8. The experimental SPCE emission angles for different concentrations of PVA and the related calculated SPR spectra.

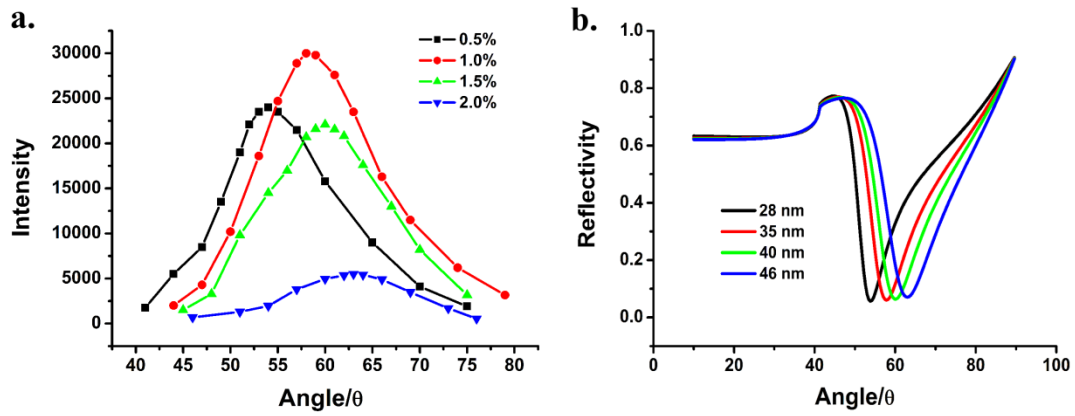


Fig. S7 (a) The experimental SPCE emission angles for different concentrations of PVA and (b) the related calculated SPR angles with given fluorophore thickness.

9. The basic SPCE properties for immunosensor based on normal SPCE.

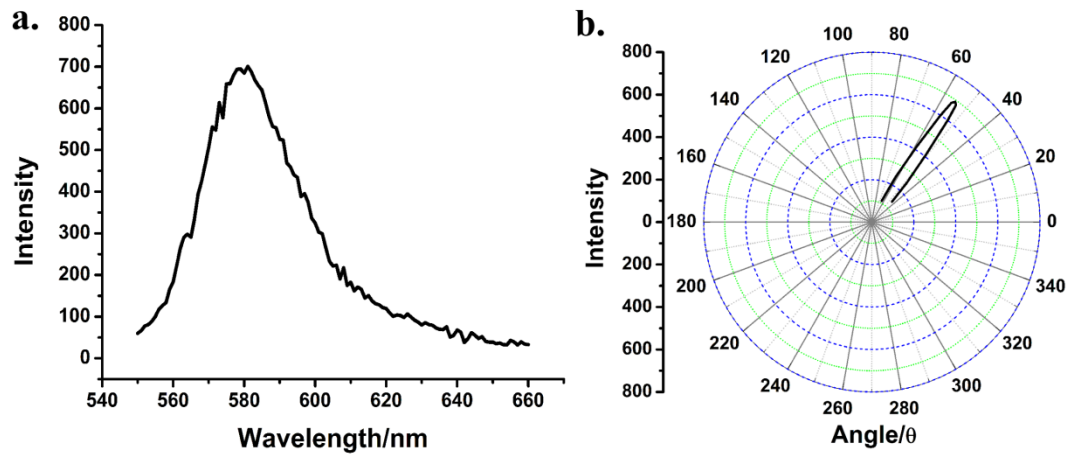


Fig. S8. (a) The polarization property and (b) the angular distribution of normal SPCE signal sensing system for concentration of 100 ng/mL.

10. The fluorescence spectrum for immunosensor based on FSE.

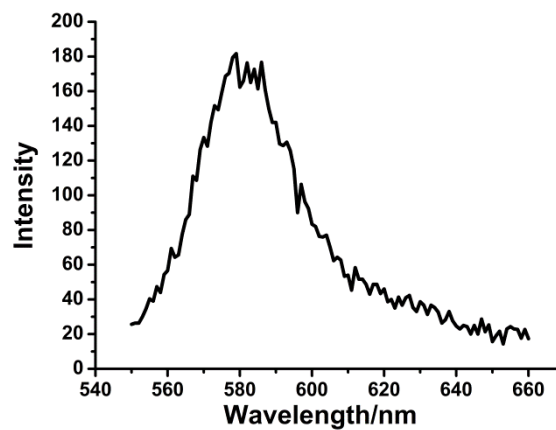


Fig. S9. The fluorescence spectrum for immunosensor based on FSE for concentration of 100

ng/mL.

11. The spectra for different concentration of goat-IgG based on CNT-assisted SPCE.

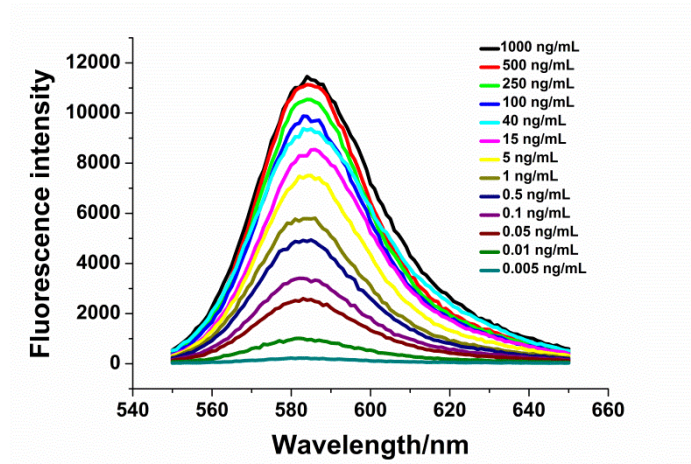


Fig. S10. The spectra of SPCE for different concentrations of goat-IgG based on CNT-assisted SPCE.

12. The spectra for different concentration of goat-IgG based on normal SPCE.

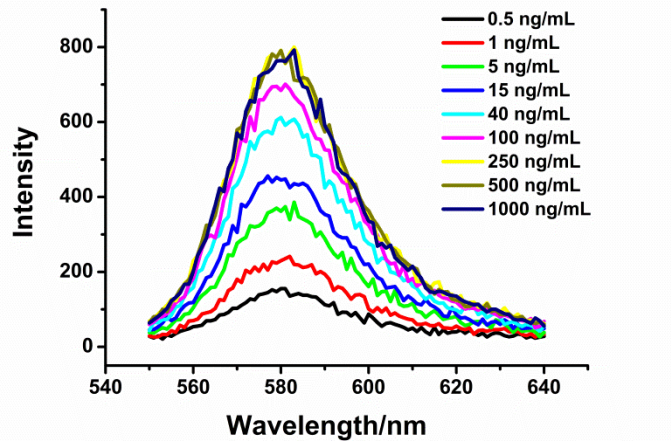


Fig. S11. The spectra for different concentrations of goat-IgG based on normal SPCE.

13. The spectra for different concentration of goat-IgG based on FSE.

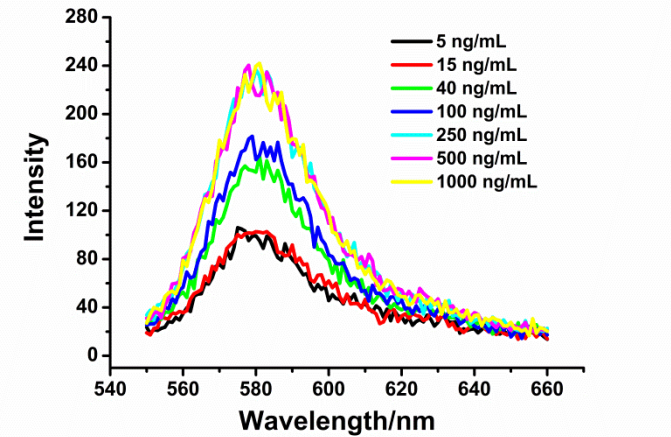


Fig. S12. The spectra for different concentrations of goat-IgG based on FSE.